62. Acyclic Tetraethynylethene Molecular Scaffolding: Multinanometer-Sized Linearly Conjugated Rods with the Poly(triacetylene) Backbone and Cross-Conjugated Expanded Dendralenes

by **Armen M. Boldi**[a]), **John Anthony**[a]), **Volker Gramlich**[b]), **Carolyn B. Knobler**[c]), **Corinne Boudon**[d]), **Jean-Paul Gisselbrecht**[d]), **Maurice Gross**[d]), and **François Diederich**[a])*

[a]) Laboratorium für Organische Chemie, Eidgenössische Technische Hochschule, ETH-Zentrum,
Universitätstrasse 16, CH-8092 Zürich
[b]) Institut für Kristallographie und Petrographie, ETH-Zentrum, Sonneggstrasse 5, CH-8092 Zürich
[c]) Department of Chemistry and Biochemistry, University of California,
Los Angeles, California 90024-1569, USA
[d]) Laboratoire d'Electrochimie et de Chimie Physique du Corps Solide, U.R.A. au C.N.R.S. n° 405,
Faculté de Chimie, Université Louis Pasteur, 1 et 4, rue Blaise Pascal, B.P. 296, F-67008 Strasbourg Cedex

(29.III.95)

Derivatives of fully cross-conjugated tetraethynylethene (3,4-diethynylhex-3-ene-1,5-diyne) **1** are versatile precursors to multinanometer-sized molecular rods with all-C-backbones. Oxidative polymerization (CuCl, *N,N,N′,N′*-tetramethylethylenediamine (TMEDA), O_2) of the *trans*-bis-deprotected *trans*-bis(triisopropylsilyl)-protected tetraethynylethene **2** yielded, after end-capping with phenylacetylene, the remarkably stable, soluble oligomers **3**–**7** with a persilylethynylated poly(triacetylene) (PTA) backbone [$-(C{\equiv}C-CR{=}CR-C{\equiv}C)_n-$] and a length of 19.4 (**3**), 26.8 (**4**), 34.3 (**5**), 41.8 (**6**), and 49.2 (**7**) Å (*Scheme 1*). These compounds underwent facile one-electron reductions with the number of reversible reduction steps being equal to the number of tetraethynylethene moieties in each molecular rod. Oxidative *Eglinton-Glaser* homo-coupling of tetraethynylethenes **8**–**10** with a single free ethynyl group provided the fully silyl-protected 3,4,9,10-tetraethynyl-substituted dodeca-3,9-diene-1,5,7,11-tetraynes **11**–**13** (*Scheme 2*) and, after alkyne deprotection, the novel hydrocarbon **14**, a $C_{20}H_6$ isomer, and its partially silyl-protected derivative **15**. Oxidative hetero-coupling between two different tetraethynylethene derivatives, one with a single and the other with two free terminal ethynyl groups, yielded the extended chromophores **16**–**21** composed of 3 or 4 tetraethynylethene moieties (*Scheme 3*). The linearly conjugated oligomers **16** and **17** with the PTA backbone are isomeric to **19** and **20**, respectively, which are members of the cross-conjugated expanded dendralenes, *i.e.*, dendralenes with butadiynediyl fragments inserted between each pair of double bonds [$-(C{\equiv}C-C({=}CR_2)-C{\equiv}C)_n-$]. The electronic absorption spectra of these compounds were compared and analyzed in terms of the competition between linear and cross-conjugation in determining the extent of π-electron delocalization. Although steric factors on π-electron conjugation remain to be clarified, this analysis strongly suggests that cross-conjugation is not an efficient mechanism for π-electron delocalization. All extended acetylenic-olefinic chromophores considered in this study exhibited remarkably high stability and did not decompose when exposed to laboratory air and light for months. In agreement with this observation, electrochemical studies demonstrated that the compounds are difficult to oxidize with the oxidation potentials in THF (0.1M $(Bu_4N)PF_6$) being higher than 1.0 V (*vs.* the ferrocene/ferrocenium couple).

1. Introduction. – Following the first preparation of the parent tetraethynylethene **1** in 1991 [1], synthetic routes to derivatives with any desired substitution and protection pattern were worked out [2] [3]. This versatile 'molecular construction kit' provided access to acetylenic C-rich nanostructure [4] precursors to all-C-networks [5] [6] and to linearly conjugated polymers with the novel poly(triacetylene) (PTA; poly(hex-1-ene-3,5-diyne)) backbone [7] [8]. In this paper, we describe *acyclic* molecular C-scaffolding and

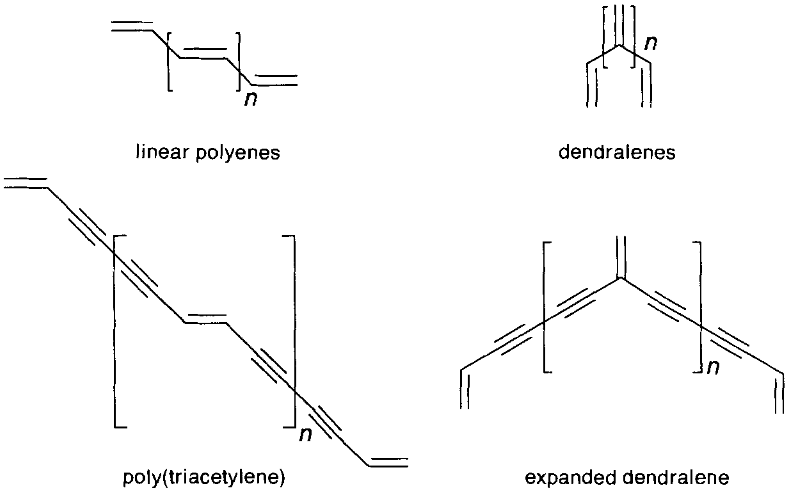

Fig. 1. *Linearly conjugated polyenes and the isomeric cross-conjugated dendralenes, and the similar structural relationship between poly(triacetylenes) and the isomeric expanded dendralenes*

show that end-capping oligomerization of *trans*-bis-deprotected *trans*-bis(triisopropylsilyl)-protected tetraethynylethene **2** [2] produces molecular wires with a PTA backbone up to 5 nm long. Molecular wires are currently under increasing investigation as components for molecular electronics devices [9]. To investigate the efficiency of cross-conjugation as a mechanism for π-electron delocalization, a series of linearly conjugated PTA oligomers and their cross-conjugated isomers of the expanded dendralene-type (*Fig. 1*) were prepared and their electronic absorption spectra compared and analyzed. Dendralenes are acyclic cross-conjugated polyenes isomeric with linear polyenes of a molecular formula C_nH_{n+2} [10]. In the expanded dendralenes, butadiynediyl fragments are inserted into each pair of double bonds. Despite a great variety of known cross-conjugated molecules, the definition of this mode of π-electron delocalization, the understanding of the underlying orbital interactions, and the extent of any resulting thermodynamic stabilization seems quite insufficient [11]. The following paper [12] reports the synthesis and properties of *macrocyclic* tetraethynylethene oligomers such as perethynylated expanded radialenes [13] and dehydroannulenes [14].

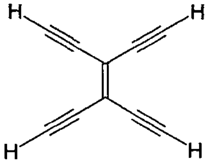

1

2. Results and Discussion. – 2.1. *Stable Soluble C-Rods with the Poly(triacetylene) Backbone by End-Capping Polymerization.* End-capping provides a versatile technique to both control oligomeric length in polymerization reactions and to enhance the stability of the products [15] [16]. When phenylacetylene was added to the oxidative polymerization of **2** under *Hay* coupling conditions in $CHCl_3$ [17], the end-capped oligomers **3**–**7** were obtained as a mixture which could be separated by chromatography (SiO_2, hexanes; *Scheme 1*). Higher oligomers could also be eluted by using $CHCl_3$ or CH_2Cl_2 but could not be separated into pure compounds. The size distribution of the oligomers strongly depended on how soon the end-capping reagent was added after the reaction was started. If an excess (6 equiv.) of phenylacetylene was added at the beginning of the reaction, monomeric **3** [2] was the only compound isolated. If addition occurred after 6–8 h, monomeric **3** through trimeric **5** were isolated in fair yields. To prepare tetrameric **6** and pentameric **7**, the reaction had to be run at least 24 h before the end-capping reagent was added.

Scheme 1. *Synthesis of Molecular Rods with a Poly(triacetylene) Backbone by End-Capping Polymerization.* The length of the individual rods originate from force-field calculations [18].

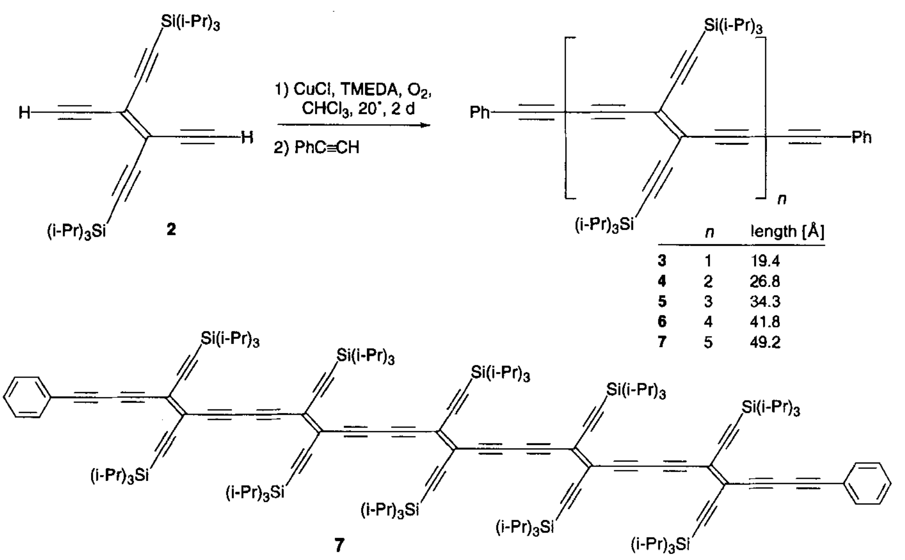

	n	length [Å]
3	1	19.4
4	2	26.8
5	3	34.3
6	4	41.8
7	5	49.2

The rods extend in length from 19.4 Å (**3**) to 49.2 Å (**7**; *cf. Scheme 1*), as shown by force-field calculations [18]. These computed values are in very good agreement with X-ray structural analyses for the shorter rods, which showed distances between the phenyl C_{para}-atoms at the termini of the rods of 19.37 Å (in **3**) [2] and 26.84 Å (in **4**; see below).

The shorter oligomers **3**–**5** are readily soluble in hexane, while the longer **6** and **7** are only moderately soluble in this hydrocarbon. All compounds **3**–**7** are readily soluble in $CHCl_3$. They are amazingly stable, high-melting materials that remain unchanged for months at room temperature when exposed to air and light. Both good solubility and high stability must be, at least in part, ascribed to the presence of the bulky laterally pendant $(i\text{-}Pr)_3Si$ groups.

In the characterization of the end-capped oligomers, matrix-assisted laser-desorption ionization time-of-flight mass spectrometry (MALDI-TOF-MS) was superior to any other mass-spectrometric techniques [13]. The spectra recorded in a 9-nitroanthracene matrix in the negative-ion mode showed mainly the molecular ions as base peaks with very minor fragmentation peaks resulting from successive losses of i-Pr groups. Interestingly, the oligomers could not be detected in the positive-ion mode, an indication for their electrochemically confirmed facile reducibility and difficult oxidizability.

The ^{13}C-NMR spectra of **3**–**7** in $CDCl_3$ were recorded with relaxation delays of up to 5 s to account for the long relaxation time particularly of the central backbone C-atoms in the longer rods. In all spectra, the alkynyl ^{13}C-resonances of the phenylacetylene end-capping groups appeared at 74 and 79 ppm, respectively, and the resonance of the directly adjacent sp-C-atom at 87 ppm. The other C-atoms of the PTA backbone appeared around 85 ppm (sp-C-atoms) and around 120 ppm (sp^2-C-atoms). The sp-C-atoms of the pendant $(i\text{-Pr})_3Si{-}C{\equiv}C$ groups resonated between 100 and 105 ppm.

Peak overlap in the ^{13}C-NMR spectra just begins in pentameric **7**, which means that the individual monomeric tetraethynylethene units in the backbone of this compound begin to resemble each other electronically. This information is important to determine what chain length of the conjugated PTA backbone is necessary to delocalize a charge carrier without that carrier experiencing end effects [19]. The charge carrier will be mobile, when it can move in either direction along a conjugated polymer chain isoenergetically, which means that the tetraethynylethene moieties on either side of the charge carrier must essentially be electronically identical. In pentameric **7**, peaks are just beginning to overlap in the alkyne region, but are still separated in the alkene region. A much larger chain length will, therefore, be required to properly delocalize a polaronic or bipolaronic unit in poly(triacetylenes).

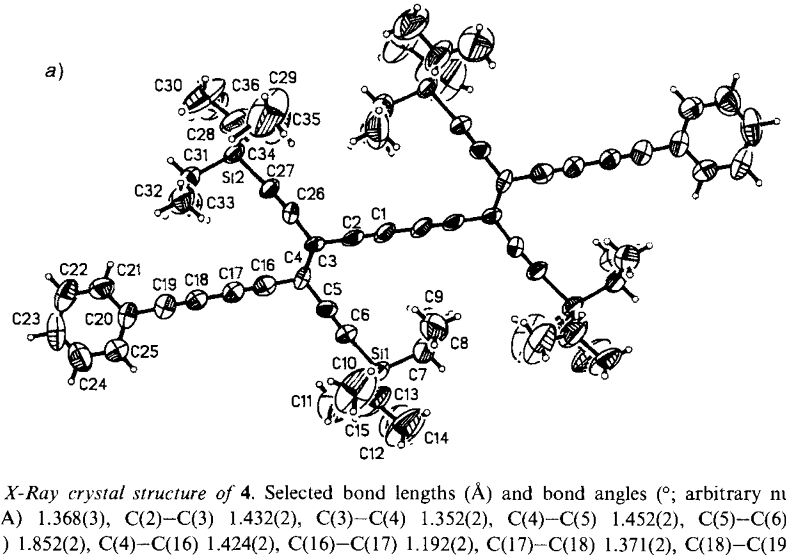

Fig. 2. a) *X-Ray crystal structure of* **4**. Selected bond lengths (Å) and bond angles (°; arbitrary numbering): C(1)–C(1A) 1.368(3), C(2)–C(3) 1.432(2), C(3)–C(4) 1.352(2), C(4)–C(5) 1.452(2), C(5)–C(6) 1.175(2), C(6)–Si(1) 1.852(2), C(4)–C(16) 1.424(2), C(16)–C(17) 1.192(2), C(17)–C(18) 1.371(2), C(18)–C(19) 1.197(2), C(19)–C(20) 1.429(2), C(3)–C(26) 1.441(2), C(26)–C(27) 1.187(2), C(27)–Si(2) 1.844(2); C(1)–C(2)–C(3) 176.4(2), C(2)–C(3)–C(4) 119.5(2), C(3)–C(4)–C(5) 121.8(1), C(4)–C(5)–C(6) 179.6(1), C(5)–C(6)–Si(1) 175.9(8), C(3)–C(4)–C(16) 121.9(2), C(4)–C(16)–C(17) 179.6(2), C(16)–C(17)–C(18) 178.1(2), C(17)–C(18)–C(19) 178.0(2), C(18)–C(19)–C(20) 178.4 (2), C(2)–C(3)–C(26) 118.1 (1), C(3)–C(26)–C(27) 176.0(1), C(26)–C(27)–Si(2) 175.8(1), C(4)–C(3)–C(26) 122.4(1).

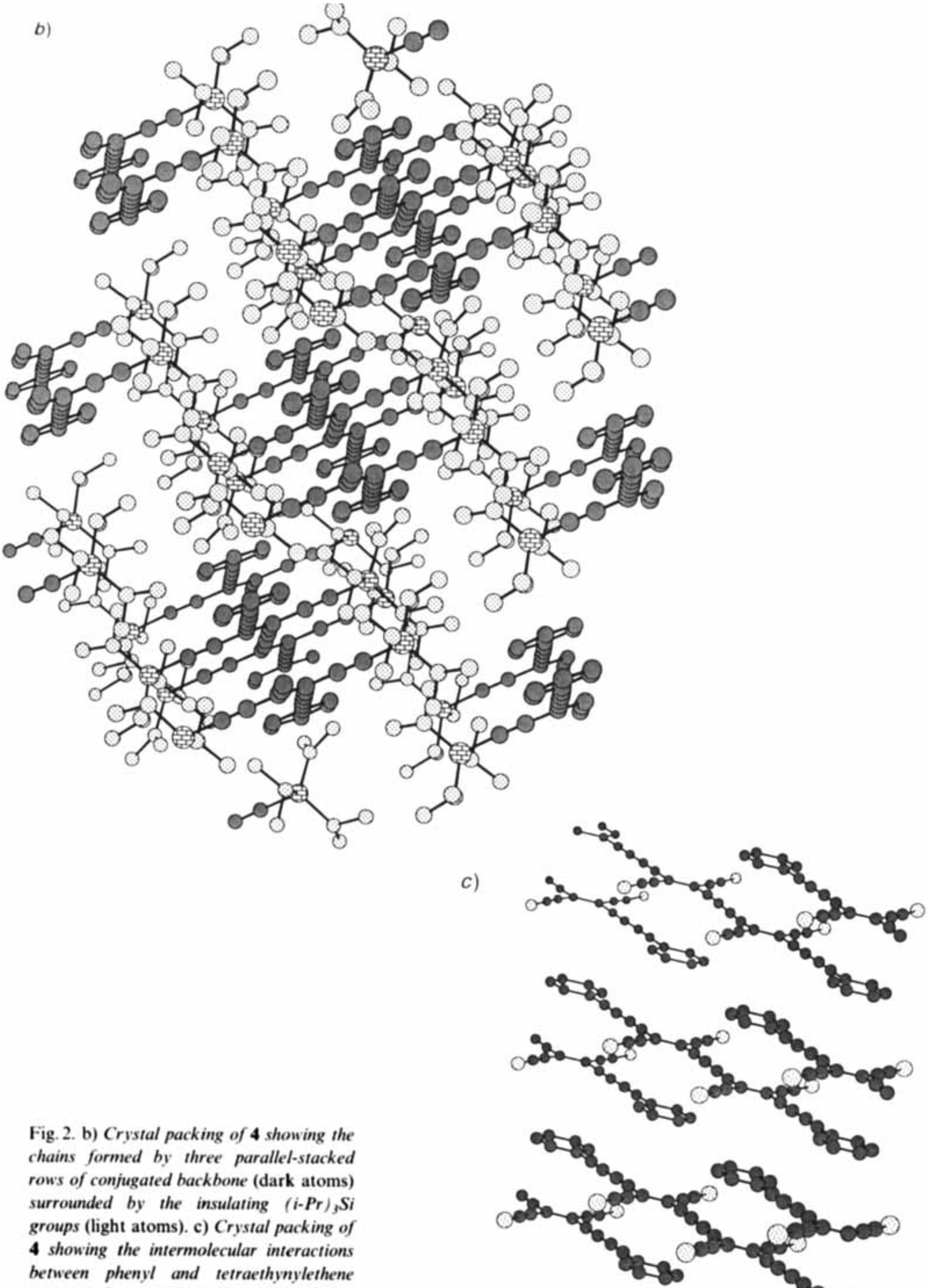

Fig. 2. b) *Crystal packing of* **4** *showing the chains formed by three parallel-stacked rows of conjugated backbone* (dark atoms) *surrounded by the insulating* $(i\text{-}Pr)_3Si$ *groups* (light atoms). c) *Crystal packing of* **4** *showing the intermolecular interactions between phenyl and tetraethynylethene moieties* (C-atoms dark, Si-atoms light).

Upon recrystallization from hexane, the shorter rods **3** and **4** formed crystals suitable for X-ray analysis [7]. The molecular structure and crystal packing of **3** have been previously reported [2]. Similarly to **3**, the conjugated C-frame of **4**, including the Ph rings, is nearly perfectly planar with a maximum deviation from the least-squares plane passing through the entire C-chromophore of only 0.03 Å (*Fig. 2a*). The distance between neighboring bulky $(i\text{-Pr})_3Si$ groups is sufficiently long (Si···Si distance of 7.56 Å) to prevent the kind of steric interactions between laterally pendant groups leading to deconjugation of the backbone in substituted polyacetylenes [20] and, to some extent, also in poly(diacetylenes) [21].

In the crystal, **4** packs in chains composed of three parallel-stacked rows of conjugated PTA backbone insulated by the $(i\text{-Pr})_3Si$ groups (*Fig. 2b*). There is electronic communication between the molecules in the three rows of each chain, with the Ph rings of one molecule stacking directly above the central C=C bonds of its neighbors' tetraethynylethene fragments (*Fig. 2c*). The centroid-centroid distance between the stacking subunits is 3.73 Å. Thus each chain can be seen as an insulated 'wire'. Recently, we showed the formation of charge-transfer complexes between tetraethynylethenes as donors and strong aromatic acceptors in the liquid phase and in the crystal [22]. This suggests that the electronic communication along insulated 'wires' such as formed by crystalline **4** (*Fig. 2b*) could be further enhanced by suitable substitution of the end-capping Ph groups.

The electronic absorption spectra, measured in $CHCl_3$, provided not only insight into the electronic characteristics of the oligomers but allowed us to correctly extrapolate important properties of longer-chain PTA's. The compounds are highly colored, with crystals changing with increasing rod length from golden-yellow (**3**), to orange-yellow (**4**), to red (**5** and **6**), and to dark-red (**7**). With increasing linear conjugation, the end absorption progresses to higher wavelength (*Fig. 3*). The observation of significant vibrational fine-structure even in the spectrum of **7** provides support for a rigid planar conjugated backbone of these rods in solution.

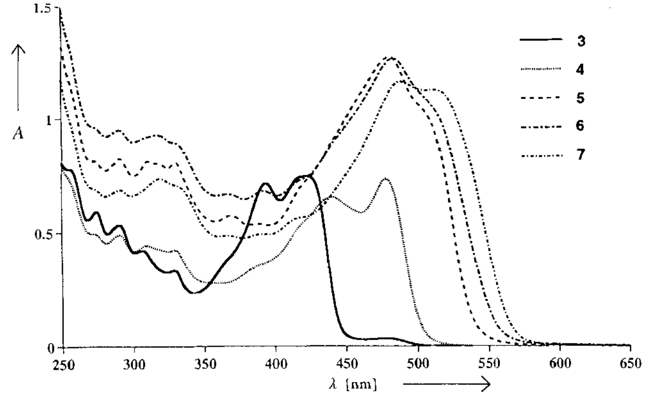

Fig. 3. *Electronic absorption spectra of* **3**–**7** *in* $CHCl_3$. $c = 2.3 \cdot 10^{-5}$ M, T 293 K.

It was shown that the longest-wavelength electronic absorption maxima for a series of oligomers can be plotted against the reciprocal oligomeric length to extrapolate the optical gap of the related longer-chain polymer [23]. Studies of this nature have been performed with polyacetylene [24], polypyrrole [25], poly(diacetylene) [26], polythiophene [15] [27], and polyphenylene [28] oligomers. The plot for oligomers **3**–**7** is linear ($r = 0.996$; *Fig. 4*), and from the intercept, the optical gap for a long-chain PTA with tetraethynylethene repeating units was predicted as 540 nm (2.25 eV). This predicted value is in very good agreement with the experimental value of 2.1 eV determined later for such longer-chain polymers [8], validifying once more the concept of studying soluble oligomers to predict and understand the properties of often insoluble polymers.

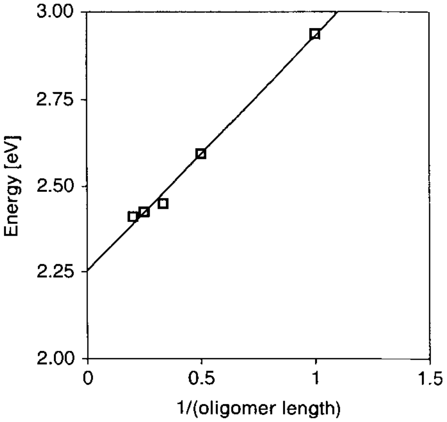

Fig. 4. *Plot of the longest-wavelength absorption maxima in the electronic absorption spectra of* **3**–**7** *as a function of the inverse of the oligomer length*

The electrochemical properties of the PTA rods were studied by polarography and cyclic voltammetry in THF (mercury working electrode; electrolyte: 0.1M $(Bu_4N)PF_6$) and were described in detail elsewhere [29]. In summary (*Table*), the rods are difficult to oxidize but undergo facile one-electron reductions. No oxidation occurs below +1.0 V *vs.* the ferrocene/ferrocenium couple (Fc/Fc^+), which helps to explain their amazing stability

Table. *Cyclic Voltammetric Reduction Characteristics of the Molecular Oligo(triacetylene) Rods* **3**–**7**, **11**, *and* **16** [29], *and of the Expanded Dendralene* **19** *on Mercury Working Electrodes in THF + 0.1* M $(Bu_4N)PF_6$

	$E_1'^{\circ}$ a)	$E_2'^{\circ}$ a)	$E_3'^{\circ}$ a)	$E_4'^{\circ}$ a)	$E_5'^{\circ}$ a)
3	−1.57	–	–	–	–
4	−1.32	−1.60	–	–	–
5	−1.17	−1.42	−2.00	–	–
6	−1.14	−1.32	−1.76	−1.99	–
7	−1.07	−1.24	−1.55	−1.65	−1.85
11	−1.52	−1.89	–	–	–
16	−1.23	−1.47b)	–	–	–
19	−1.36c)	−1.74c)	–	–	–

a) V *vs.* Fc/Fc^+, formal reduction potential $E'^{\circ} = (E_{p_a} + E_{p_c})/2$. b) Peak potential E_{p_c} for irreversible reduction. c) On Pt electrode.

when exposed for months to laboratory air. In the series **3**–**7**, the number of reversible one-electron reduction steps corresponds to the number of tetraethynylethene moieties in each rod. As the oligomer length increases, the first reduction occurs at increasingly less negative potentials (E'° at −1.57 V for **3** and −1.07 V for **7** *vs.* Fc/Fc$^+$ in THF). Thus, the electrochemistry of **3**–**7**, with their unsaturated all-C-backbones, resembles that of the fullerenes which also undergo facile multiple one-electron reductions but are difficult to oxidize [30]. This suggests a general property of unsaturated all-C-matter as will be further discussed in the following paper [12].

2.2. *Synthesis of Small Per(silylethynyl)ated Poly(triacetylene) Oligomers and Their Cross-Conjugated Isomers of the Expanded-Dendralene Type.* Although the oxidative acetylenic coupling under *Hay* conditions with the CuCl/TMEDA complex in acetone under air was successfully used in the end-capping polymerization leading to **3**–**7**, higher yields of acyclic tetraethynylethene oligomers were generally obtained by using the *Eglinton-Glaser* coupling conditions with anhydrous Cu(OAc)$_2$ in pyridine or pyridine/

Scheme 2. *Synthesis and Deprotection of Dimeric Tetraethynylethenes*

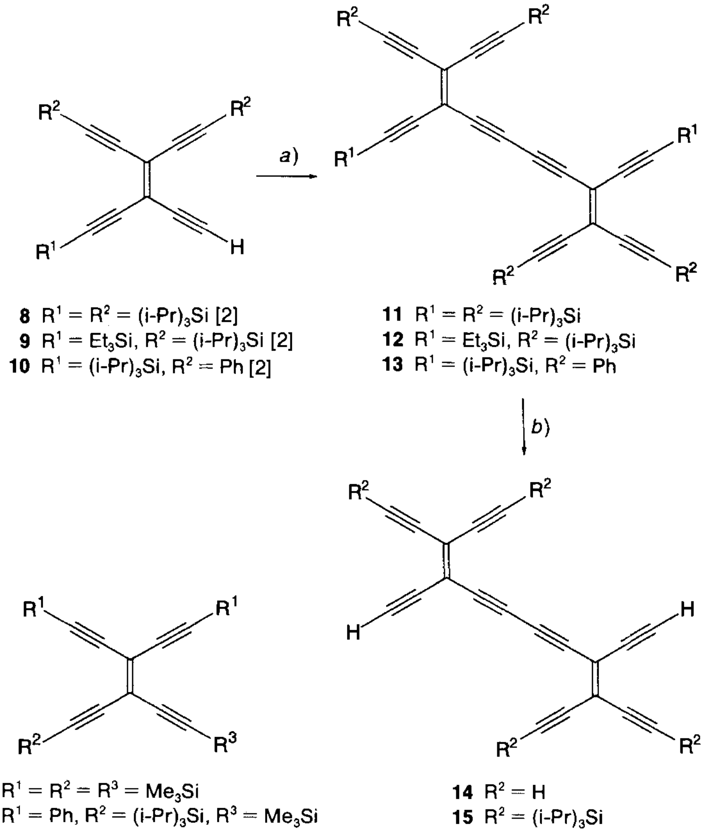

8 R^1 = R^2 = (i-Pr)$_3$Si [2]
9 R^1 = Et$_3$Si, R^2 = (i-Pr)$_3$Si [2]
10 R^1 = (i-Pr)$_3$Si, R^2 = Ph [2]

11 R^1 = R^2 = (i-Pr)$_3$Si
12 R^1 = Et$_3$Si, R^2 = (i-Pr)$_3$Si
13 R^1 = (i-Pr)$_3$Si, R^2 = Ph

29 R^1 = R^2 = R^3 = Me$_3$Si
30 R^1 = Ph, R^2 = (i-Pr)$_3$Si, R^3 = Me$_3$Si

14 R^2 = H
15 R^2 = (i-Pr)$_3$Si

a) Anh. Cu(OAc)$_2$, pyridine (for **11**) or pyridine/benzene 1:1 (for **12** and **13**); 59% (**11**), 64% (**12**), 72% (**13**).
b) For **14** (unstable in the solid state): Bu$_4$NF, wet THF; for **15**: K$_2$CO$_3$, MeOH/THF 1:1; 67%.

benzene under inert gas atmosphere [31]. Thus, the dimeric compounds **11–13** were formed from **8–10** in good yields (59–72%) as high-melting stable solids (*Scheme 2*). The structure of **11** was confirmed in an X-ray crystal-structure analysis (*Fig. 5*) [32] that revealed a nearly planar molecule with a maximum deviation from the least-squares plane through the dimeric framework including the six Si-atoms of 0.21(3) Å. Similar to the structure of **4**, the two ethene moieties in crystalline **11** adopt the *'transoid'* alignment with respect to the central butadiyne moiety. The eighteen (i-Pr) groups are highly disordered, which prevented refinement of the structure beyond $R = 0.169$ ($R_w = 0.178$) [32].

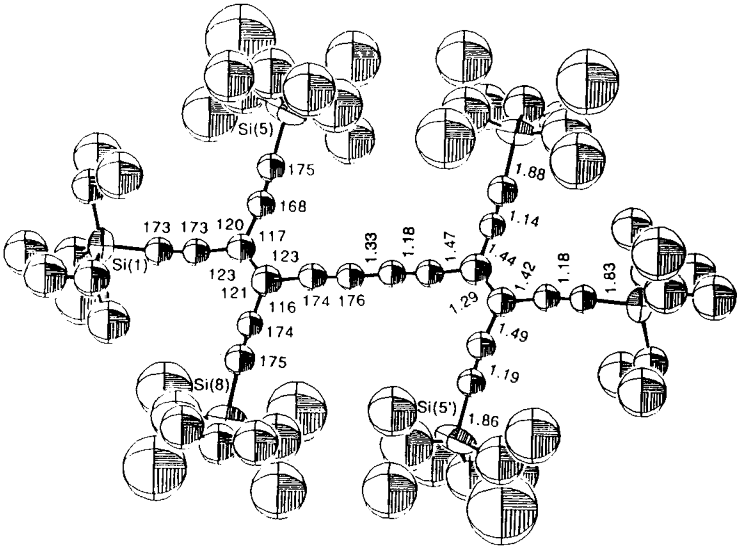

Fig. 5. *X-Ray crystal structure of* **11**

Deprotection of **11** with Bu_4NF in wet THF afforded the parent hexaethynyl derivative **14**, the first $C_{20}H_6$ hydrocarbon, which was moderately stable in pentane solution (*Scheme 2*). At room temperature, even in the absence of O_2 and light, evaporation of the solvent yielded a solid that rapidly turned into a black material which was insoluble in all common organic solvents. The ^{1}H-NMR spectrum of **14** in $(CD_3)_2CO$ manifested three characteristic singlets of equal intensity for the terminal alkyne protons at 4.51, 4.57, and 4.60 ppm. No *Bergman* cycloaromatization reaction [33] was observed upon refluxing **14** in toluene. Regioselective deprotection of **12** with K_2CO_3 in MeOH/THF afforded the diethynyl derivative **15** as a semi-stable oil which served as a building block in the construction of expanded radialenes [12] [13]. As noted previously [2], then stability of tetraethynylethene derivative decreases rapidly with increasing number of free terminal acetylenes.

Since *Cadiot-Chodkiewicz* hetero-coupling reactions [31b] [34] with brominated tetraethynylethenes was unsuccessful [2], the longer oligo(triacetylenes) **16–18** and their isomeric counterparts **19–21** of the expanded-dendralene type were prepared by mixed coupling of differentially substituted tetraethynylethenes using the *Eglinton-Glaser* method. Thus, reaction of **23** (2 equiv.), freshly prepared by deprotection of **22** [2], with

24 (1 equiv.) [2] afforded small amounts of the oligomers **16**–**18** in addition to dimer **11** produced by homo-coupling of **23** (*Scheme 3*). Similarly, reaction of **23** (2 equiv.) with **26** (1 equiv.), freshly obtained by deprotection of **25** [2], afforded small quantities of the expanded dendralenes **19** and **20** in addition to homo-coupling product **11**. Finally, the

Scheme 3. *Synthesis of the Per(silylethynyl)ated Oligo(triacetylenes)* **16**–**18**, *of the Per(silylethynyl)ated Expanded Dendralenes* **19** *and* **20**, *and of the Differentially Protected Perethynylated Expanded Dendralene* **21**

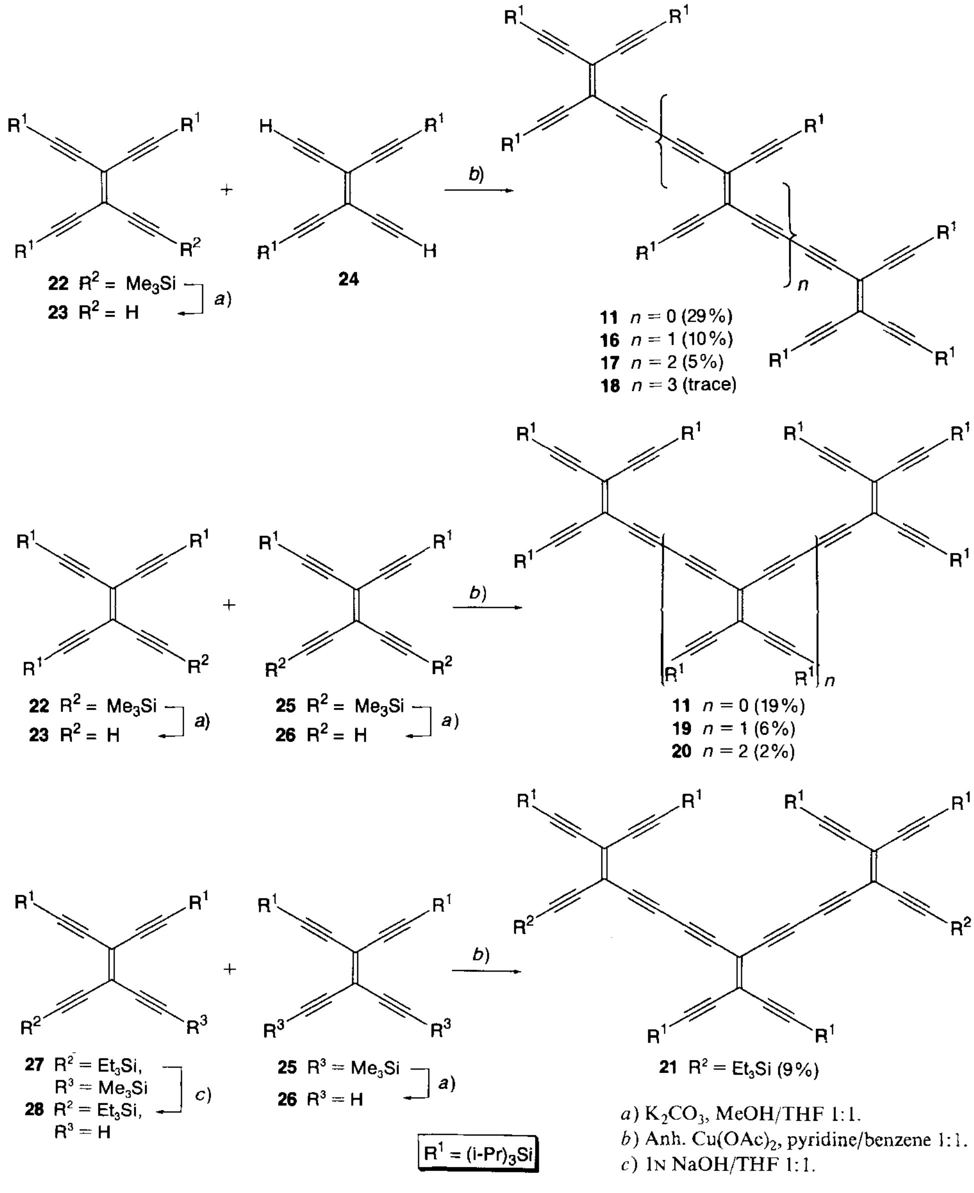

a) K_2CO_3, MeOH/THF 1:1.
b) Anh. $Cu(OAc)_2$, pyridine/benzene 1:1.
c) 1N NaOH/THF 1:1.

differentially protected expanded dendralene **21**, a precursor to the expanded radialenes [12], was obtained in 9% yield by hetero-coupling of **28** (2 equiv.) and **26** (1 equiv.), which were both freshly prepared by deprotection of **27** and **25**, respectively.

In the characterization of the extended chromophores **16**–**21**, laser-desorption time-of-flight mass spectrometry (LD-TOF-MS) and ^{13}C-NMR spectroscopy provided particularly valuable information. *Fig. 6* shows the LD-TOF-MS of the two expanded dendralenes **19** and **20** recorded in the linear negative-ion mode with a mass resolution $m/\Delta m \approx 200$. Spectra of similar quality were measured for **16**–**18** and **21** and demonstrated the purity of the materials as well as essentially complete lack of fragmentation. In the ^{13}C-NMR spectra, the signals of the C-backbone appeared in ranges similar to those assigned for the backbone resonances in **3**–**7**: the sp^2-C-atoms are found around 120 ppm, the sp-C-atoms of the $R_3Si{-}C{\equiv}C$ groups around 105 ppm, and the sp-C-atoms of the butadiyndiyl fragments between 80 and 85 ppm.

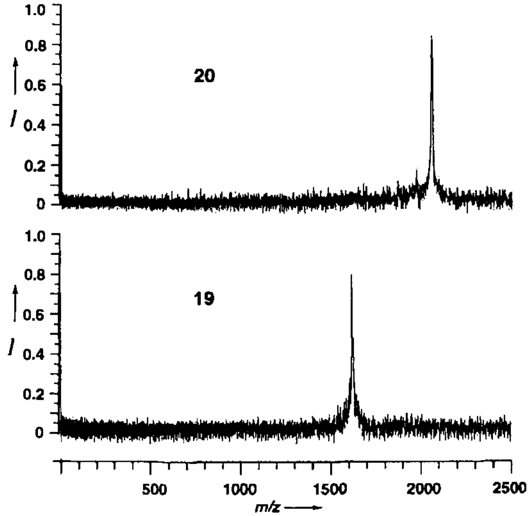

Fig. 6. *Laser-desorption time-of-flight mass spectra of the expanded dendralenes* **19** (bottom) *and* **20** (top). Recorded in the linear negative-ion mode.

2.3. *Evaluation of Linear and Cross-Conjugation Effects by Electronic Absorption Spectroscopy.* The extension of the π-electron delocalization in the planar dimeric chromophores **11** and **13** becomes clearly visible in the comparison of their electronic absorption spectra to those of the monomeric tetraethynylethenes **29** [2] and **30** [2] (see *Scheme 2*). The end absorption of **11** appears above 450 nm (*Fig. 7*), and the longest-wavelength band at λ_{max} 432 nm is bathochromically shifted by 82 nm compared to the lowest-energy absorption in **29** (λ_{max} 350 nm). The longest-wavelength band in **13** (λ_{max} 466 nm) is shifted to exactly the same extent as compared to the corresponding band in **30** (λ_{max} 384 nm). In agreement with the planar molecular structure found by X-ray analysis, the UV/VIS spectrum of **11** exhibits significant vibrational fine structure. π-Electron delocalization is enhanced by the Ph groups in **13** that shows a bathochromically shifted

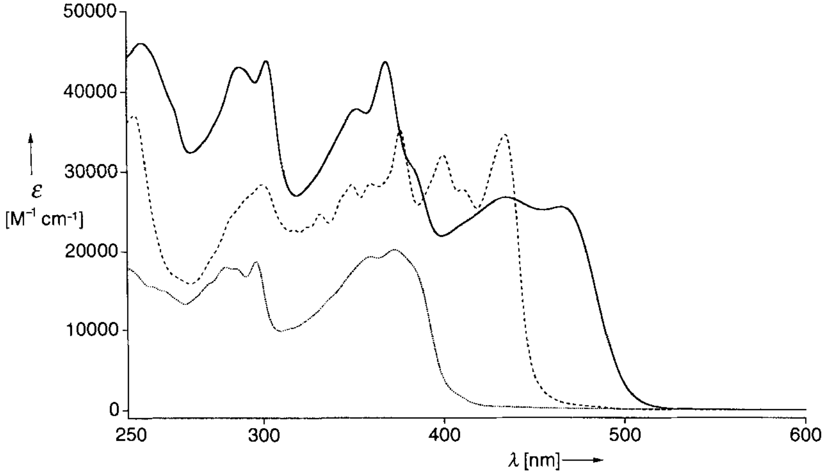

Fig. 7. *Electronic absorption spectra of* **30** (⋯⋯), **11** (------), *and* **13** (——) *in hexane. T* 298 K.

end absorption compared to **11**. Broadly spaced absorption bands are diagnostic of the Ph derivatives **30** and **13**. In both compounds, two sets of bands appear at nearly identical positions, one at 270–300 nm and one at 320–400 nm. We assign these bands to the absorption by the linearly conjugated chromophore $Ph{-}C{\equiv}C{-}CR{=}CR{-}C{\equiv}C{-}Si(i\text{-}Pr)_3$ which is present in both systems. In addition, the dimeric compound **13** shows a long-wavelength band above 400 nm and extending to above 500 nm. This absorption must be assigned to the longest linearly conjugated chromophore in **13**, which corresponds to the $Ph{-}C{\equiv}C{-}CR{=}CR{-}C{\equiv}C{-}C{\equiv}C{-}CR{=}CR{-}C{\equiv}C{-}Ph$ (1,12-diphenyldodeca-3,9-diene-1,5,7,11-tetrayne) fragment.

In the series of oligo(triacetylenes) **11** and **16**–**17**, similar to the phenylacetylene end-capped series **3**–**7**, an increasing bathochromic shift of the longest-wavelength band and the end absorption with increasing linear conjugation length along the molecular backbone is observed (*Fig. 8*). In sharp contrast, the absorption of the expanded dendralenes **19** and **20** is not at all bathochromically shifted compared to the spectrum of **11** (*Fig. 9*). Rather, nearly identical spectra with regard to absorption wavelength and vibrational fine structure are observed for all three compounds. The extinction coefficients of the absorption bands of **19** are nearly twice those of **11**. The absorptions of the more extended chromophore **20** are slightly broader with molar extinction coefficients between those calculated for **11** and **19**.

We explain the surprising findings in the expanded-dendralene series by limited π-electron delocalization in **19** and **20**, that appears to extend efficiently only through the longest linearly conjugated fragment which corresponds exactly to the dodeca-3,9-diene-1,5,7,11-tetrayne backbone in **11**. Apparently, cross-conjugation across the central bifurcating tetraethynylethene moieties in **19** and **20** is not a very efficient mechanism for π-electron delocalization. However, steric reasons for the reduced π-electron conjugation cannot be fully excluded. Both preliminary computer and CPK modeling show that the steric repulsion between the bulky interior $(i\text{-}Pr)_3Si$ groups distorts the chromophores out of planarity. We are currently conducting higher-level calculations [35] to determine the

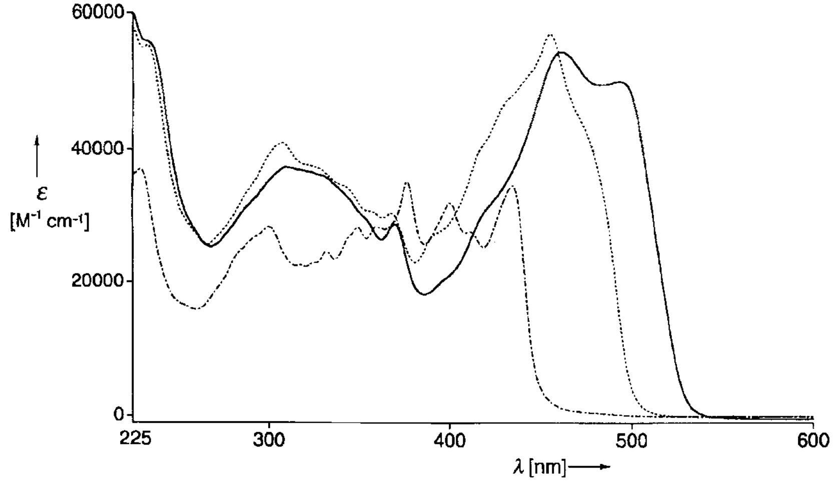

Fig. 8. *Electronic absorption spectra or* **11** (·-·-·-·-), **16** (------), *and* **17** (——) *in hexane. T* 298 K.

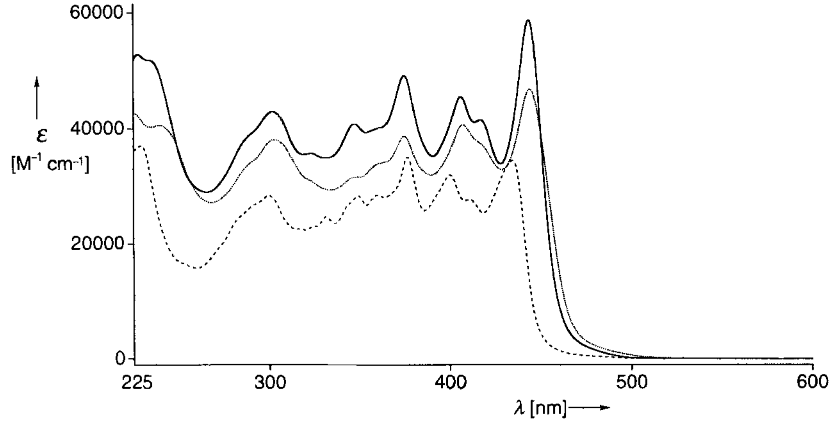

Fig. 9. *Electronic absorption spectra of* **11** (------), **19** (——), *and* **20** (······) *in hexane. T* 298 K.

extent of distortion from planarity and its influence on conjugation, a sensitive subject in view of the two sets of in-plane and out-of-plane acetylenic π-orbitals that could participate in the conjugation in sterically distorted systems. Regardless, the pronounced vibrational fine structure of the electronic absorption spectra suggests that the expanded dendralenes **19** and **20**, like the planar oligo(triacetylenes) **3**–**7**, **11**, and **16**–**17**, have strong conformational preferences and are not very flexible.

Strong evidence for the reduced π-electron delocalization in the expanded dendralene **19** as compared to the PTA isomer **16** was also provided in the electrochemical studies. Under cyclic voltammetric conditions, the cross-conjugated system **19** underwent two reversible one-electron reductions at significantly more negative potential than **16** (see above, *Table*) which can be readily explained by the reduced π-electron delocalization in the expanded dendralene.

3. Conclusions. – Starting from a versatile tetraethynylethene 'molecular construction kit' [2], a series of oligomers with either poly(triacetylene) (PTA) or expanded-dendralene backbones were prepared by end-capping polymerization or by hetero-coupling of differentially protected tetraethynylethene derivatives. Despite the presence of up to 22 C≡C bonds (in **7**), the highly colored oligomers are amazingly stable, high-melting compounds that can be stored at room temperature in the air for prolonged periods of time. Electrochemical studies demonstrated that the unexpected stability of the new materials is partially due to resistance to oxidation; like fullerenes, the tetraethynylethene oligomers prefer multiple reversible one-electron reductions, and this redox behavior seems to be a characteristic feature of unsaturated C-matter. Another important contribution to the kinetic stability of these new nanomaterials comes from the laterally pendant bulky $(i\text{-}Pr)_3Si$ groups which also provide high solubility to the compounds. Electronic absorption measurements of the oligo(triacetylene) rods **3**–**7** allowed accurate prediction of the optical gap of the corresponding longer-chain polymers. Because of their remarkable stability, such oligomers could become useful components in molecular electronics. Their length can be further extended without loss of stability. To make contact with these 'molecular wires', any desired substituent can be attached to the ends of the rods by changing the end-capping reagent. The lateral silyl groups can be exchanged for other substituents to allow attachment to substrates such as silicon wafers.

For the expanded dendralenes **19**–**21**, modeling reveals that steric compression between $(i\text{-}Pr)_3Si\text{-}C{\equiv}C$ groups exists, although its influence on planarity and π-conjugation of the backbone remains to be determined in X-ray crystallographic and computational studies. The electronic absorption spectra of these compounds clearly demonstrate that the extent of π-electron delocalization is limited to the longest linearly conjugated π-electron fragment, a 3,4,9,10-tetraalkynyl-substituted dodeca-3,9-diene-1,5,7,11-tetrayne. Although steric effects could be important, we believe that the electronic spectra provide strong evidence for inefficient cross-conjugation in the expanded dendralenes. It is hoped that future careful experimental and computational studies on **19**–**21** and other cross-conjugated systems such as expanded radialenes described in the following paper [12] will provide further insight into the poorly understood, yet so frequent phenomenon of cross-conjugation in extended π-systems. It should be noted that buckminsterfullerene (C_{60}) is best described as a cross-conjugated molecule with [5] radialene substructures and that the electronic structure of graphite may also be viewed as cross-conjugated. We speculate that limitation of π-electron delocalization due to inefficient cross-conjugation may be a general stabilizing principle of unsaturated C-based matter.

This work was supported at UCLA by the *U.S. National Science Foundation* and the *Office of Naval Research* and at ETHZ by a grant from the *Swiss National Science Foundation* and ETH setup funds. *J.A.* was supported at UCLA by a graduate-student fellowship from the *American Chemical Society*. We thank Dr. *W. Amrein* for help with the LD-TOF and MALDI-TOF mass spectra.

Experimental Part

General. See [2]. All reactions were performed in standard glassware under an inert atmosphere of N_2 or Ar, except when noted otherwise. Anh. $MgSO_4$ was used as the drying agent after workup in all the experiments. Evaporation and concentration was done at water-aspirator pressure, followed by pumping under high vacuum (10^{-3} Torr). If not indicated otherwise, ^1H- and ^{13}C-NMR spectra were recorded in $CDCl_3$. DEI-MS: desorption electron-impact mass spectrometry.

Laser-Desorption Time-of-Flight Mass Spectrometry. Mass spectra were obtained using the *Bruker Reflex* instrument with a N_2 laser system (337 nm, > 175 µJ/pulse, 3-ns pulse width) to desorb and ionize analyte molecules in laser-desorption (LD) or matrix-assisted laser-desorption ionization (MALDI) mode. For LD-TOF, the analyte in toluene or CH_2Cl_2 was deposited onto the center of the probe tip and dried under vacuum. For MALDI-TOF, 9-nitroanthracene was used as the matrix. All reported data were acquired using the linear negative-ion mode at −15 kV. Laser attenuation adjusted the laser power. All spectra were processed and printed using the XMASS program on a *SUN* workstation. The average mass resolution ($m/\Delta m$) was 200.

End-Capping Polymerization of **2**. To a soln. of **2** (2.2 g, 5.0 mmol) in $CHCl_3$ open to air was added CuCl (100 mg, 1.0 mmol) and TMEDA (1.54 g, 2.0 ml, 13 mmol). The reaction was followed by TLC (SiO_2, hexane) until the desired oligomeric products had formed. To prepare significant quantities of pentameric **7**, *e.g.*, the reaction was run for 2 d. Phenylacetylene (9.3 g, 10 ml, 91 mmol) was then added along with CuCl (50 mg, 0.5 mmol) and TMEDA (0.385 g, 0.5 ml, 3.3 mmol). After stirring for 12 h, the solvent was evaporated and the resulting solid dissolved in hot hexane. This soln. was passed through a thick pad of SiO_2 which was flushed with hexane to elute a mixture of 1,4-diphenylbuta-1,3-diyne, **3**, and **4**, and subsequently with $CHCl_3$ to elute the mixture of higher oligomers. The hexane fraction was concentrated to 100 ml and then passed through a second plug of SiO_2. Only the bright-yellow fraction was collected and evaporated to give, after recrystallization from hexane, golden-yellow crystals of monomeric **3** (0.89 g, 28%; m.p. 142° ([2]: 142–143°)). The $CHCl_3$ fraction from the first plug filtration was evaporated and the darkred solid redissolved in hexane and flash chromatographed (SiO_2, hexane) to give highly colored fractions of **4**–**7**.

*(*E,E*)-1,16-Diphenyl-5,6,11,12-tetrakis[(triisopropylsilyl)ethynyl]hexadeca-5,11-diene-1,3,7,9,13,15-hexayne* (**4**). Yield 886 mg (33%). Orange-yellow crystals. M.p. 180° (dec.). UV/VIS ($CHCl_3$): 270 (21 000), 290 (21 000), 309 (19 000), 329 (18 000), 384 (sh, 15 000), 440 (28 000), 478 (31 000). IR (KBr): 2200 (C≡C). ^1H-NMR (200 MHz): 1.156 (*s*, 42 H); 1.17 (*s*, 42 H); 7.36 (*m*, 6 H); 7.50 (*m*, 4 H). ^{13}C-NMR (125.8 MHz): 11.17; 11.22; 18.57; 18.60; 74.17; 78.86; 83.83; 84.29; 85.04; 87.24; 101.4; 101.7; 104.4; 105.0; 119.5; 120.6; 121.5; 128.5; 129.6; 132.5. MALDI-TOF-MS: 1073 (100, M^-). Anal. calc. for $C_{72}H_{94}Si_4 \cdot 0.5\ CHCl_3$ (1131.58): C 76.95, H 8.42; found: C 76.90, H 8.21. X-Ray: see *Fig. 2*.

*(*E,E,E*)-1,22-Diphenyl-5,6,11,12,17,18-hexakis[(triisopropylsilyl)ethynyl]docosa-5,11,17-triene-1,3,7,9,13,15,19,21-octayne* (**5**). Yield 403 mg (16%). Red crystals. M.p. 245° (dec.). UV/VIS ($CHCl_3$): 274 (40 500), 290 (41 000), 311 (40 100), 330 (39 900), 368 (28 600), 480 (63 800), 506 (51 500). IR (KBr): 2179, 2177, 2133 (C≡C). ^1H-NMR (200 MHz): 1.13 (*s*, 42 H); 1.14 (*s*, 42 H); 1.16 (*s*, 42 H); 7.37 (*m*, 6 H); 7.5 (*m*, 4 H). ^{13}C-NMR (125.7 MHz): 11.16; 11.21; 18.56; 18.60; 74.15; 78.85; 83.90; 84.15; 84.25; 84.75; 85.10; 87.29; 101.3; 101.4; 101.7; 104.5; 105.1; 105.2; 119.4; 120.1; 120.7; 121.5; 128.5; 129.6; 132.5. MALDI-TOF-MS: 1507 (100, M^-), 1463 ($[M - C_3H_7]^-$), 1419 ($[M - 2C_3H_7]^-$). Anal. calc. for $C_{100}H_{136}Si_6$ (1506.71): C 79.72, H 9.10; found: C 79.89, H 9.03.

*(*E,E,E,E*)-1,28-Diphenyl-5,6,11,12,17,18,23,24-octakis[(triisopropylsilyl)ethynyl]octacosa-5,11,17,23-tetraene-1,3,7,9,13,15,19,21,25,27-decayne* (**6**). Yield 170 mg (7%). Red crystals. M.p. 250° (dec.). UV/VIS ($CHCl_3$): 272 (40 900), 291 (40 300), 317 (39 400), 327 (38 000), 366 (28 300), 392 (28 900), 416 (sh, 30 600), 484 (53 600), 511 (sh, 44 600). IR (KBr): 2200, 2177, 2133 (C≡C). ^1H-NMR (200 MHz): 1.117 (*s*, 42 H); 1.119 (*s*, 42 H); 1.123 (*s*, 42 H); 1.14 (*s*, 42 H); 7.37 (*m*, 6 H); 7.5 (*m*, 4 H). ^{13}C-NMR (125.8 MHz): 11.19; 11.25; 18.54; 18.57; 74.17; 78.89; 83.90; 84.20; 84.21; 84.25; 84.67; 84.79; 85.10; 87.29; 101.31; 101.35; 101.5; 101.7; 104.5; 105.1; 105.3; 105.35; 119.3; 120.0; 120.1; 120.7; 121.5; 128.5; 129.6; 132.5. MALDI-TOF-MS: 1937 (100, M^-). Anal. calc. for $C_{128}H_{178}Si_8 \cdot CHCl_3$ (2060.91): C 75.18, H 8.75; found: C 74.97, H 8.54.

*(*E,E,E,E,E*)-1,34-Diphenyl-5,6,11,12,17,18,23,24,29,30-decakis[(triisopropylsilyl)ethynyl]tetratriaconta-5,11,17,23,29-pentaene-1,3,7,9,13,15,19,21,25,27,31,33-dodecayne* (**7**). Yield 48 mg (2%). Dark red crystals. M.p. 250° (dec.). UV/VIS ($CHCl_3$): 290 (25 300), 320 (25 800), 329 (25 700), 367 (sh, 18 200), 390 (sh, 17 800), 419 (sh, 19 700), 490 (37 500), 514 (38 700). IR (KBr): 2199, 2168, 2152, 2130 (C≡C). ^1H-NMR (200 MHz): 1.116 (br. *s*, 84 H); 1.118 (*s*, 42 H); 1.123 (*s*, 42 H); 1.142 (*s*, 42 H); 7.37 (*m*, 6 H); 7.5 (*m*, 4 H). ^{13}C-NMR (125.8 MHz): 11.23; 11.30; 11.46; 18.58; 18.61; 74.21; 78.93; 83.899; 84.191; 84.229; 84.289; 84.646; 84.665; 84.737; 84.801; 85.108; 87.296; 101.299 (2×); 101.337; 101.443; 101.712; 101.712; 104.506; 105.128; 105.329; 105.344; 119.328; 119.980; 120.105; 120.196; 120.693; 121.560; 128.5; 129.6; 132.5. MALDI-TOF-MS: 2376 (M^-). Anal. calc. for $C_{156}H_{220}Si_{10} \cdot 0.5\ CHCl_3$ (2436.03): C 77.16, H 9.12; found: C 76.95, H 9.21.

1,12-Bis(triisopropylsilyl)-3,4,9,10-tetrakis[(triisopropylsilyl)ethynyl]dodeca-3,9-diene-1,5,7,11-tetrayne (**11**). To a soln. of **8** (266 mg, 0.448 mmol) [2] in pyridine (45 ml) was added anh. $Cu(OAc)_2$ (1.6 g, 8.81 mmol). The mixture was stirred for 20 h at r.t. and then poured into pentane (250 ml) and 30% aq. $CuSO_4$ soln. (500 ml). The aq. layer was extracted with pentane (1×), and the combined org. layers were washed with 30% aq. $CuSO_4$ soln. (2 × 500 ml), H_2O (250 ml), and sat. aq. NaCl soln. (250 ml). The brownish solid obtained after drying was resuspended in pentane and filtered through a plug of SiO_2 for FC. Evaporation and recrystallization (MeOH/CH_2Cl_2) yielded **11** (156 mg, 59%). Yellow solid. M.p. 236–239° (dec.). UV/VIS (hexane): 223 (sh, 36 800), 228

(37700), 253 (sh, 17500), 283 (sh, 25500), 291 (sh, 27800), 299 (29600), 316 (23200), 324 (23600), 331 (25300), 343 (sh, 27600), 347 (sh, 29000), 358 (28900), 374 (35600), 398 (33000), 408 (28300), 432 (35500). IR (KBr): 2156, 2125 (C≡C). ^{1}H-NMR (360 MHz): 1.07 (*s*, 126 H). ^{13}C-NMR (90.6 MHz): 11.13; 11.20; 11.24; 18.53; 18.61; 18.65; 82.34; 82.98; 101.55; 103.14; 104.34; 103.64; 103.70; 105.05; 115.91; 120.80. DEI-MS: 1183 (100, M^+). HR-MS: 1182.8480 (M^+, $C_{74}H_{126}Si_6^+$; calc. 1182.8475). Anal. calc. for $C_{74}H_{126}Si_6$ (1184.34): C 75.05, H 10.72; found: C 75.11, H 10.50. X-Ray (crystals from hexane/EtOH): *Fig. 5*.

4,9-Bis[(triethylsilyl)ethynyl]-1,12-bis(triisopropylsilyl)-3,10-bis[(triisopropylsilyl)ethynyl]dodeca-3,9-diene-1,5,7,11-tetrayne (**12**). To a soln. of **9** (159 mg, 0.289 mmol) [2] in benzene/pyridine 1:1 (50 ml) was added anh. $Cu(OAc)_2$ (503 mg, 2.769 mmol), and the mixture was stirred overnight at r.t. Workup as described for **11** afforded an oil which was filtered through a plug (SiO_2 for FC, hexane): **12** (101 mg, 64%). Yellow solid. M.p. 231–233° (dec.). UV/VIS (hexane): 214 (36800), 225 (34600), 233 (sh, 29000), 253 (sh, 15300), 281 (23300), 290 (26900), 301 (26900), 323 (18900), 331 (19100), 350 (21700), 360 (21900), 377 (29800), 401 (36900), 412 (30400), 436 (48400). IR (KBr): 2159, 2126 (C≡C). ^{1}H-NMR (500 MHz): 0.65 (*q*, *J* = 7.9, 18 H); 1.01 (*t*, *J* = 7.9, 12 H); 1.11 (*s*, 84 H). ^{13}C-NMR (75.5 MHz): 4.19; 7.46; 11.22; 18.55; 18.62; 82.50; 83.06; 100.77; 103.51; 103.58 (2×); 103.77; 104.88; 116.12; 121.15. DEI-MS: 1099 (100, M^+). Anal. calc. for $C_{68}H_{114}Si_6$ (1100.18): C 74.24, H 10.44; found: C 73.98, H 10.32.

4,9-Bis[(triisopropylsilyl)ethynyl]-1,12-diphenyl-3,10-bis(phenylethynyl]dodeca-3,9-diene-1,5,7,11-tetrayne (**13**). To a soln. of **10** (113 mg, 0.261 mmol) in benzene/pyridine 1:1 (25 ml) was added anh. $Cu(OAc)_2$ (447 mg, 2.46 mmol), and the mixture was stirred at r.t. overnight. Workup as described for **11** afforded an oil which was passed through a plug (SiO_2 for FC, hexane): **13** (80.8 mg, 72%). Red solid. M.p. 134–135°. UV/VIS (hexane): 233 (46100), 251 (37900), 287 (43000), 302 (43800), 353 (37800), 368 (43600), 385 (29900), 435 (26800), 466 (25500). IR (film): 2187, 2137 (C≡C). ^{1}H-NMR (200 MHz): 1.13 (*s*, 42 H); 7.27–7.38 (*m*, 12 H); 7.50–7.56 (*m*, 8 H). ^{13}C-NMR (75.5 MHz): 11.29; 18.65; 82.68; 83.82; 87.08; 87.39; 100.12; 100.73; 102.06; 103.13; 115.18; 121.23; 122.07; 122.33; 128.25 (2×); 128.31, 129.22; 131.91; 132.08. DEI-MS: 862 (M^+). Anal. calc. for $C_{62}H_{62}Si_2$ (863.35): C 86.26, H 7.24; found: C 86.15, H 7.53.

3,4,9,10-Tetraethynyldodeca-3,9-diene-1,5,7,11-tetrayne (**14**). To **11** (20.8 mg, 0.018 mmol) was added wet THF (5 ml) and 1.0M Bu_4NF in THF (0.2 ml, 0.2 mmol). After stirring for 15 min at r.t., the mixture was poured into pentane/H_2O 1:1 and washed with H_2O (3×) and sat. aq. NaCl soln. (1×). Evaporation yielded a yellow oil that rapidly turned black. ^{1}H-NMR (360 MHz, $(CD_3)_2CO$): 4.51 (*s*, 2 H); 4.57 (*s*, 2 H); 4.60 (*s*, 2 H).

4,9-Diethynyl-1,12-bis(triisopropylsilyl)-3,10-bis[(triisopropylsilyl)ethynyl]dodeca-3,9-diene-1,5,7,11-tetrayne (**15**). To **12** (36.3 mg, 0.033 mmol) was added MeOH/THF 1:1 (4 ml) and K_2CO_3 (35 mg, 0.253 mmol). After stirring for 1 h at r.t., TLC (reversed-phase SiO_2, CH_2Cl_2/MeCN 2:1) showed the presence of deprotected **15** (R_f 0.56). The mixture was poured into pentane/H_2O 1:1 and washed with H_2O and sat. aq. NaCl soln. Drying and evaporation gave **15** (19.4 mg, 67%). Unstable oil. IR (film): 3304 (≡C–H), 2128, 2099 (C≡C). ^{1}H-NMR (500 MHz): 1.10 (*s*, 42 H); 1.11 (*s*, 42 H); 3.49 (*s*, 2 H). ^{13}C-NMR (500 MHz): 11.2; 18.5; 79.2; 82.9; 83.1; 86.7; 102.7; 103.0; 104.5; 105.1; 115.1; 122.6. LD-TOF-MS: 872 (M^-).

1,18-Bis(triisopropylsilyl)-3,4,9,10,15,16-hexakis[(triisopropylsilyl)ethynyl]octadeca-3,9,15-triene-1,5,7,11,13,17-hexayne (**16**), *1,24-Bis(triisopropylsilyl)-3,4,9,10,15,16,21,22-octakis[(triisopropylsilyl)ethynyl]tetracosa-3,9,15,21-tetraene-1,5,7,11,13,17,19,23-octayne* (**17**), *and 1,30-Bis(triisopropylsilyl)-3,4,9,10,15,16,21,22,27,28-decakis[(triisopropylsilyl)ethynyl]triaconta-3,9,15,21,27-pentaene-1,5,7,11,13,17,19,23,25,29-decayne* (**18**). To a soln. of **22** (236.2 mg, 0.355 mmol) was added K_2CO_3 (491 mg, 3.55 mmol) in MeOH/THF (1:1 (50 ml). After stirring at r.t. for 15 min, the mixture was poured into pentane/H_2O 1:1. Washing the org. phase with H_2O and sat. aq. $NaHCO_3$ soln. followed by evaporation afforded **23** as an oil [2] which was used without further purification. To this oil and **24** (40.94 mg, 0.0937 mmol) [2] was added benzene/pyridine 1:1 (40 ml) and anh. $Cu(OAc)_2$ (725 mg, 3.991 mmol). The mixture was stirred for 22 h at r.t. and then poured into 30% aq. $CuSO_4$ soln. and hexane. The org. layer was washed with 30% aq. $CuSO_4$ soln. (3×), H_2O, and sat. aq. NaCl soln. After drying and evaporation, the resulting orange solid was subjected to FC (SiO_2, hexane) to give four fractions. *Fr. 1* yielded **11** (61.5 mg, 29%).

Fr. 2 gave **16** (15.8 mg, 10%). Stable orange solid. M.p. 257–258°. UV/VIS (hexane): 207 (sh, 91500), 225 (sh, 58000), 235 (sh, 54700), 308 (41000), 328 (sh, 37100), 344 (sh, 34100), 368 (30500), 390 (sh, 26900), 417 (sh, 40100), 431 (sh, 46900), 455 (sh, 56900), 475 (42400), 479 (sh, 39600). IR (film): 2155, 2118 (C≡C). ^{1}H-NMR (300 MHz): 1.10, 1.11 (2*s*, 168 H). ^{13}C-NMR (75.5 MHz): 11.17; 11.24; 18.55; 18.60; 82.21; 82.66; 84.51; 84.70; 101.32; 101.51; 103.34; 103.65; 103.70; 104.81; 105.47; 115.71; 119.89; 121.31. LD-TOF-MS: 1619 (100, M^-). Anal. calc. for $C_{102}H_{168}Si_8$ (1619.16): C 75.66, H 10.46; found: C 75.92, H 10.62.

Fr. 3 gave **17** (4.6 mg, 5%). Stable red solid. M.p. > 260°. UV/VIS (hexane): 216 (sh, 70000), 236 (sh, 55100), 314 (37100), 370 (28900), 394 (sh, 19900), 418 (sh, 30100), 462 (54400), 497 (49600). IR (KBr): 2156, 2125 (C≡C). ^{1}H-NMR (500 MHz): 1.09, 1.10 (2*s*, 210 H). ^{13}C-NMR (125.8 MHz): 10.91; 11.14; 11.15; 11.20; 11.23; 11.36;

18.51; 18.55; 18.59; 18.63; 82.14; 82.60; 84.11; 84.51; 84.68; 84.94; 101.28 (2×); 101.45; 103.36; 103.61; 103.68 (2×); 105.01; 105.09; 105.52; 115.64; 119.68; 120.31; 121.35. LD-TOF-MS: 2055 (100, M^-). Anal. calc. for $C_{130}H_{210}Si_{10}$ (2053.98): C 76.02, H 10.31; found: C 76.27, H 10.75.

Fr. 4 gave a trace of **18**. Stable red solid. UV/VIS (hexane): 234 (sh), 304, 331, 354, 369, 396, 472, 499. IR (film): 2155, 2124 (C≡C). ^{1}H-NMR (300 MHz): 1.087 (*s*); 1.090 (*s*); 1.103 (*s*). LD-TOF-MS: 2486 (100, M^-, $C_{158}H_{252}Si_{12}$).

1,17-Bis(triisopropylsilyl)-3,4,14,15-tetrakis[(triisopropylsilyl)ethynyl]-9-{3-(triisopropylsilyl)-1-[(triisopropylsilyl)ethynyl]prop-2-ynylidene}heptadeca-3,14-diene-1,5,7,10,12,16-hexayne (**19**) *and 1,22-Bis(triisopropylsilyl)-3,4,19,20-tetrakis[(triisopropylsilyl)ethynyl]-9,14-bis{3-(triisopropylsilyl)-1-[(triisopropylsilyl)ethynyl]-prop-2-ynylidene}-docosa-3,19-diene-1,5,7,10,12,15,17,21-octayne* (**20**). To a soln. of **22** (701 mg, 1.054 mmol) [2] and **25** (191 mg, 0.329 mmol) [2] was added K_2CO_3 (843 mg, 6.10 mmol) in MeOH/THF 1:1 (100 ml). After stirring at r.t. for 15 min, the mixture was poured into pentane and H_2O. Washing with H_2O and sat. aq. $NaHCO_3$ soln. gave an oily mixture of **23** [2] and **26** [2] which was carried onto the next step without further purification. To a vigorously stirred soln. of this oil in pyridine/benzene (50 ml) was added anh. $Cu(OAc)_2$ (2.162 g, 11.90 mmol). After stirring at r.t. for 25 h, the mixture was poured into 30% aq. $CuSO_4$ soln. and hexane. The org. layer was washed with 30% aq. $CuSO_4$ (3×), H_2O, and sat. aq. NaCl soln. and evaporated and the dark yellow oil chromatographed (reversed-phase SiO_2, CH_2Cl_2/MeCN 2:1) to give three fractions, *Fr. 1* contained **11** (118 mg, 19%).

Fr. 2 yielded **19** (33 mg, 6%). Stable yellow solid. M.p. 116–118°. UV/VIS (hexane): 213 (sh, 48400), 227 (52800), 236 (sh, 51400), 287 (sh, 38300), 302 (43000), 324 (sh, 35800), 347 (40900), 361 (sh, 40200), 375 (49200), 406 (45600), 418 (41500), 444 (58900). IR (film): 2153, 2127 (C≡C). ^{1}H-NMR (500 MHz): 1.087, 1.091 (2*s*, 168 H). ^{13}C-NMR (125.8 MHz): 11.19; 11.20; 11.23; 11.25; 18.54; 18.55; 18.63; 18.67; 81.33; 81.95; 83.54; 83.78; 101.51; 103.09; 103.36; 103.53; 103.68; 103.72; 105.19; 106.02; 115.68; 115.72; 121.10; 122.83. LD-TOF-MS: 1619 (100, M^-). Anal. calc. for $C_{102}H_{168}Si_8$ (1619.16): C 75.66, H 10.46; found: C 75.67, H 10.31.

Fr. 3 afforded **20** (5.5 mg, 2%). Stable yellow solid. M.p. 127–128°. UV/VIS (hexane): 226 (42600), 239 (40600), 290 (sh, 34100), 303 (38100), 323 (sh, 31100), 346 (31500), 360 (33900), 375 (38800), 407 (40800), 416 (sh, 37700), 444 (47000). IR (film): 2124 (C≡C). ^{1}H-NMR (300 MHz): 1.087, 1.091, 1.100 (3*s*, 210 H). ^{13}C-NMR (125,7 MHz): 11.15; 11.17; 11.19; 11.21; 18.50; 18.51; 18.59; 18.63; 81.20; 81.90; 81.93; 83.05; 83.64; 83.87; 101.40; 102.95; 103.06; 103.30; 103.51; 103.64; 103.77; 105.25; 106.13; 106.32; 115.39; 115.65; 121.24; 123.12. LD-TOF-MS: 2054 (100, M^-). Anal. calc. for $C_{130}H_{210}Si_{10}$ (2053.98): C 76.02, H 10.31; found: C 75.81; H 10.37.

4,14-Bis[(triethylsilyl)ethynyl]-1,17-bis(triisopropylsilyl)-3,15-bis[(triisopropylsilyl)ethynyl]-9-{3-(triisopropylsilyl)-1-[(triisopropylsilyl)ethynyl]prop-2-ynylidene}heptadeca-3,14-diene-1,5,7,10,12,16-hexayne (**21**). To a soln. of **27** (108.9 mg, 0.175 mmol) [2] in MeOH/THF 1:1 (100 ml) were added 8 drops of 1N NaOH. After stirring at r.t. for 2.5 min, the mixture was poured into pentane/H_2O. Washing with H_2O and sat. aq. $NaHCO_3$ soln. gave **28** [2] as an oil that was carried onto the next step without further purification. In a separate flask, a mixture of **25** (31.2 mg, 0.054 mmol) [2] and K_2CO_3 (63 mg, 0.456 mmol) in MeOH/THF 1:1 (50 ml) was stirred at r.t. for 1 h, then poured into pentane and H_2O. Washing with H_2O and sat. aq. $NaHCO_3$ soln. gave **26** [2] as an oil that was carried onto the next step without further purification. To a vigorously stirred mixture of the freshly prepared **26** and **28** in pyridine/benzene 1:1 (10 ml) was added anh. $Cu(OAc)_2$ (259 mg, 1.426 mmol). After stirring at r.t. overnight, the mixture was poured into 30% aq. $CuSO_4$ soln. and hexane. Washing the org. layer with 30% aq. $CuSO_4$ soln. (3×), H_2O, and sat. aq. NaCl soln. afforded, after evaporation, a dark yellow oil which was passed through a plug (SiO_2 for FC, hexane). Reversed-phase chromatography (CH_2Cl_2/MeCN 2:1) gave as a 1st fraction dimeric material and, in a 2nd fraction, **21** (7.1 mg, 9%). Stable yellow oil. M.p. 146–147°. UV/VIS (hexane): 226 (49700), 235 (sh, 47000), 288 (sh, 36000), 301 (40100), 324 (32400), 347 (37800), 362 (sh, 37400), 375 (45400), 406 (45500), 417 (41400), 444 (59000). IR (film): 2152, 2129 (C≡C). ^{1}H-NMR (500 MHz): 0.63 (*q*, *J* = 7.9, 18 H); 0.99 (*t*, *J* = 7.9, 12 H); 1.09, 1.10, 1.11 (3*s*, 126 H). ^{13}C-NMR (125.7 MHz): 4.19; 7.46; 11.21; 18.54; 18.62; 81.43; 82.17; 83.53; 83.64; 100.75; 103.08; 103.36; 103.54; 103.93; 103.96; 104.98; 106.09; 115.66; 115.92; 121.29; 123.07. LD-TOF-MS: 1535 (100, M^-). Anal. calc. for $C_{96}H_{156}Si_8$ (1535.00): C 75.12, H 10.24; found: C 75.14, H 10.22.

REFERENCES

[1] Y. Rubin, C. B. Knobler, F. Diederich, *Angew. Chem.* **1991**, *103*, 708; *ibid. Int. Ed.* **1991**, *30*, 698.

[2] J. Anthony, A. M. Boldi, Y. Rubin, M. Hobi, V. Gramlich, C. B. Knobler, P. Seiler, F. Diederich, *Helv. Chim. Acta* **1995**, *78*, 13.

[3] H. Hopf, M. Kreutzer, P. G. Jones, *Chem. Ber.* **1991**, *124*, 1471.

[4] Z. Wu, S. Lee, J. S. Moore, *J. Am. Chem. Soc.* **1992**, *114*, 8730; J. Zhang, J. S. Moore, *ibid.* **1994**, *116*, 2655; Z.

Xu, M. Kahr, K.L. Walker, C.L. Wilkins J.S. Moore, *ibid.* **1994**, *116*, 4537; J. Zhang, D.J. Pesak, J.L. Ludwick, J.S. Moore, *ibid.* **1994**, *116*, 4227.

[5] F. Diederich, *Nature (London)* **1994**, *369*, 199.

[6] U.H.F. Bunz, *Angew. Chem.* **1994**, *106*, 1127; *ibid. Int. Ed.* **1994**, *33*, 1073.

[7] J.A. Anthony, C. Boudon, F. Diederich, J.-P. Gisselbrecht, V. Gramlich, M. Gross, M. Hobi, P. Seiler, *Angew. Chem.* **1994**, *106*, 794; *ibid. Int. Ed.* **1994**, *33*, 763.

[8] M. Schreiber, J. Anthony, F. Diederich, M.E. Spahr, R. Nesper, M. Hubrich, F. Bommeli, L. Degiorgi, P. Wachter, P. Kaatz, C. Bosshard, P. Günter, M. Colussi, U.W. Suter, C. Boudon, J.-P. Gisselbrecht, M. Gross, *Adv. Mater.* **1994**, *6*, 786.

[9] R. Eastmond, T.R. Johnson, D.R.M. Walton, *Tetrahedron* **1972**, *28*, 4601; G. Tourillon, F. Garnier, *J. Electroanal. Chem.* **1981**, *135*, 173; J.-M. Lehn, *Angew. Chem.* **1988**, *100*, 91; *ibid. Int. Ed.* **1988**, *27*, 89; J.M. Lehn, *Makromol. Chem., Macromol. Symp.* **1993**, *69*, 1; M.A. Reed, *Sci. Am.* **1993**, *268*, 98; A.J. Aviram, *J. Am. Chem. Soc.* **1988**, *110*, 5687; D. Ofer, R.M. Crooks, M.S. Wrighton, *ibid.* **1990**, *112*, 7869; P. Kaszynski, A.C. Friedli, J. Michl, *ibid.* **1992**, *114*, 601, and ref. cit. therein; J. Müller, K. Base, T.F. Magnera, J. Michl, *ibid.* **1992**, *114*, 9721; X. Yang, W. Jiang, C.B. Knobler, M.F. Hawthorne, *ibid.* **1992**, *114*, 9719; J.S. Schumm, D.L. Pearson, J.M. Tour, *Angew. Chem.* **1994**, *106*, 1445; *ibid. Int. Ed.* **1994**, *33*, 1360; J.M. Tour, *Adv. Mater.* **1994**, *6*, 190; J.E.C. Wiegelmann, U.H.F. Bunz, *Organometallics* **1988**, *7*, 789; U.H.F. Bunz, M. Altmann, *Makromol. Chem., Rapid Commun.* **1994**, *15*, 785.

[10] H. Hopf, *Angew. Chem.* **1984**, *96*, 947; *ibid. Int. Ed.* **1984**, *23*, 948.

[11] M.J.S. Dewar, *J. Chem. Soc.* **1952**, 3544; N.F. Phelan, M. Orchin, *J. Chem. Educ.* **1968**, *45*, 633; P. Gund, *ibid.* **1972**, *49*, 100; J. Klein, *Tetrahedron* **1983**, *39*, 2733; N. Tyutyulkov, F. Dietz, K. Müllen, M. Baumgarten, S. Karabunarliev, *Chem. Phys.* **1994**, *189*, 83.

[12] J. Anthony, A.M. Boldi, C. Boudon, J.-P. Gisselbrecht, M. Gross, P. Seiler, C.B. Knobler, F. Diederich, *Helv. Chim. Acta* **1995**, *78*, 797.

[13] A.M. Boldi, F. Diederich, *Angew. Chem.* **1994**, *106*, 482; *ibid. Int. Ed.* **1994**, *33*, 468.

[14] J. Anthony, C.B. Knobler, F. Diederich, *Angew. Chem.* **1993**, *105*, 437; *ibid. Int. Ed.* **1993**, *32*, 406.

[15] P. Bäuerle, *Adv. Mater.* **1992**, *4*, 102.

[16] T.X. Neenan, M.R. Callstrom, L.M. Scarmoutzos, K.R. Stewart, G.M. Whitesides, V.R. Howes, *Macromolecules* **1988**, *21*, 3525.

[17] A.S. Hay, *J. Org. Chem.* **1962**, *27*, 3320.

[18] 'CVFF Force Field', Biosym Technologies, San Diego, 1993.

[19] R.R. Chance, D.S. Boudreaux, H. Eckhardt, R.L. Elsenbaumer, J.E. Frommer, J.L. Brédas, R. Silbey, 'Quantum Chemistry of Polymers – Solid State Aspects', Plenum Publishing Corp., New York, 1994, p. 221; C.C. Ku, R. Liepnis, 'Electrical Properties of Polymers', Hanser, Munich, 1987, Chapt. 5; P.J.S. Foot, N.C. Billingham, P.D. Calvert, *Synth. Met.* **1966**, *16*, 265.

[20] J.L. Brédas, R.R. Chance, R.H. Baughman, R. Silbey, *J. Chem. Phys.* **1982**, *76*, 3673.

[21] R.H. Baughman, J.L. Brédas, R.R. Chance, R.L. Elsenbaumer, L.W. Shacklette, *Chem. Rev.* **1982**, *82*, 209; K.C. Lim, A.J. Heeger, *J. Chem. Phys.* **1985**, *82*, 522.

[22] F. Diederich, D. Philp, P. Seiler, *J. Chem. Soc., Chem. Commun.* **1994**, 205; D. Philp, V. Gramlich, P. Seiler, F. Diederich, *J. Chem. Soc., Perkin Trans. 2*, in press.

[23] J. L. Brédas, R. Silbey, D.S. Boudreaux, R.R. Chance, *J. Am. Chem. Soc.* **1983**, *105*, 6555.

[24] K. Knoll, R.R. Schrock, *J. Am. Chem. Soc.* **1989**, *111*, 7989.

[25] G. Zotti, S. Martina, G. Wegner, A.-D. Schlüter, *Adv. Mater.* **1992**, *4*, 798.

[26] F. Wudl, S.P. Bitler, *J. Am. Chem. Soc.* **1986**, *108*, 4685.

[27] J.M. Tour, R. Wu, *Macromolecules* **1992**, *25*, 1901.

[28] R.K. Khanna, Y.M. Jiang, D. Creed, *J. Am. Chem. Soc.* **1991**, *113*, 5451.

[29] C. Boudon, J.-P. Gisselbrecht, M. Gross, J. Anthony, A.M. Boldi, R. Faust, T. Lange, D. Philp, J.-D. van Loon, F. Diederich, *J. Electroanal. Chem.*, in press.

[30] Q. Xie, F. Arias, L. Echegoyen, *J. Am. Chem. Soc.* **1993**, *115*, 9818.

[31] a) O.M. Behr, G. Eglinton, A.R. Galbraith, R.A. Raphael, *J. Chem. Soc.* **1960**, 3614; b) K. Sonogashira, in 'Comprehensive Organic Synthesis', Ed. B.M. Trost, Pergamon, New York, 1991, Vol. 3, pp. 551–561; c) D. O'Krongly, S.R. Denmeade, M.Y. Chiang, R. Breslow, *J. Am. Chem. Soc.* **1985**, *107*, 5544.

[32] A.M. Boldi, J. Anthony, C.B. Knobler, F. Diederich, *Angew. Chem.* **1992**, *104*, 1270; *ibid. Int. Ed.* **1992**, *31*, 1240.

[33] R.G. Bergman, *Acc. Chem. Res.* **1973**, *6*, 25.

[34] W. Chodkievicz, *Ann. Chim. (Paris)* **1957**, *2*, 819.

[35] H.-P. Lüthi, A. Hilger, F. Diederich, unpublished results.